

REFERENCE: DY05

THE METHOD OF GENERALIZED FLOQUET THEORY APPLIED TO FLAP-LAG  
DYNAMICS WITH INFLOW

Xin Wang and David A. Peters  
Washington University  
St. Louis, MO 63130

The method of Generalized Floquet Theory is introduced in which Floquet analysis can be performed in the absence of a complete set of independent state excitations or independent state measurements. In the new method, an arbitrary set of excitations and measurements can be used. The space of excitations is enriched by consideration of measurements at each blade passage as an excitation for the next passage. The set of measurements is enhanced by utilization of time-shifted states (i.e., pseudo-states). The entire set of excitations and outputs is finally converted to a best estimate of the Floquet Transition Matrix by Singular Value Decomposition. The New methodology is successfully applied to the flap-lag dynamics of a 4-bladed lifting rotor with dynamic wake.

NOTATION

a	Two-dimensional lift curve slope, rad <sup>-1</sup>
[A(t)]	Periodic eigenvectors
c	Blade chord, ft
$C_{d_0}$	Blade profile drag coefficient
$C_T$	Thrust coefficient
$C_\zeta$	Lead-lag hinge damping, ft-lb-sec/rad
[D(t)]	Matrix of periodic coefficients
$I_b$	Blade flapping inertia, slug-ft <sup>2</sup>
[J]	Jacobian matrix
k	Number of time shifts plus one
$K_\beta$	Flap hinge spring stiffness at $\theta=0$ , ft-lb/rad
$K_\zeta$	Lead-Lag hinge spring stiffness at $\theta=0$ , ft-lb/rad
n	Time delay factor
N	Number of states
p	Dimensionless rotating flapping frequency at $\theta=0$
P	Stiffness Parameter, p <sup>2</sup>
Q	Number of blades
[Q]	Floquet Transition matrix
R	Blade radius, ft
[R]	Relation matrix
t	Time, sec
T	Period
W	Stiffness parameter
$x_i$	States
{x}	State vector

$X_{Old}$	Old state vector
$X_{New}$	New pseudo-state vector
Z	Stiffness parameter
$\beta$	Flap angle, positive up, rad
$\beta_{pc}$	Pre-cone angle, rad
$\gamma$	Lock number, $\rho ac R^4 / I_b$
$\Delta t$	Time delay, nondimensional time
$\delta t$	Smallest nondimensional time unit used in calculation or sampling rate
$\delta x$	Perturbation of states
$\zeta$	Lead-lag angle, positive forward, rad
$\eta_i$	Characteristic Floquet exponents
$\theta$	Pitch angle, rad
$\lambda_k$	Real part of exponents
$\mu$	Nominal advance ratio, nondimensional flow parallel to disk
$\sigma$	Rotor solidity, $Qc/(\pi R)$
$\psi$	Azimuth angle, rad, $=\Omega t$
$\Omega$	System rotational speed, rad/s

INTRODUCTION

The method of Floquet Theory is the most powerful and popular method used to analyze the dynamic stability of helicopter rotors. Lewis [1] was the first to use Floquet Theory on helicopter rotors; Peters and Hohenemser [2] were the first to implement it with packaged time-marching and eigenvalue routines. Simplicity and accuracy made Floquet Theory popular. The only requirements to do

Floquet analysis are time-marching tools and eigenvalue solvers. The improvement of computers also makes accurate Floquet analysis possible for systems up to several hundred states. A paper by Peters [3] introduced the McNulty Method (Fast Floquet Theory) to improve Floquet analysis of a Q-bladed rotor system. The symmetry of Q-bladed rotors is utilized in Fast Floquet Theory to reduce time-marching CPU time by  $1/Q$ . It also helps to improve the accuracy of eigenvalues and make the identification of eigenvalues easier.

Another paper by Peters and Su [4] mentions the effect of hidden aerodynamic states on Floquet analysis. Failure to perturb hidden states can cause large errors in the results, especially when hidden states are near blade dynamic states in the root-locus plane. This turns out to be a serious problem in Floquet analysis because aerodynamic states are often both hidden and in close proximity to dynamic poles. Another problem with Floquet Theory is that it is not readily applicable to experimental data. This is because conventional Floquet Theory requires that each state be excited and measured independently. With experimental data, however, one is severely limited both in how a system can be excited and in what states can be measured.

In this paper, we offer a method that can generalize conventional Floquet analysis so that it can be applicable to numerical or experimental data that may be neither complete nor independent, Ref. [5]. Preliminary results can be found in Ref. [6]. In the generalized theory, the space of excitations is increased by consideration of data after each blade passage to be a new excitation. The space of states is increased by the utilization of time-shifted states (i.e., pseudo-states) at every blade passage. With this method, the column and row rank of the excitations and measurements can be increased. Singular Value Decomposition can then be used to identify the Least-Squares best approximation to the Floquet Transition Matrix. Further research on the pseudo-state method is carried out to make this method simpler, more accurate, and more practical. Several other concepts are also used to improve the accuracy of this method. Data and error analyses are also given.

Most of the codes used are programmed in Matlab.

## ROTOR MODEL AND NUMERICAL METHOD

A typical hingeless rotor-blade system can be modeled as blades connected to a shaft by torsion springs ( $K_\beta$  and  $K_\zeta$ ) and dampers ( $C_\zeta$ ). In order to control the rotor, a pitch angle  $\theta$  is also applied along the blade axis, Ref. [7]. The azimuth angle is

$\psi = \Omega t$ . The motion of each blade is uniquely determined in the rotating coordinate system by three Euler angles:  $\beta$ ,  $\zeta$  and  $\theta$ .  $\beta$  is the flap angle,  $\zeta$  is the lead-lag angle, and  $\theta$  is prescribed. A one-bladed rotor model without inflow and a four-bladed rotor model with 4-harmonics of dynamic inflow are used in later calculations.

The dynamic inflow model is the dynamic wake model, Ref.[8].

The major numerical method used to solve the nonlinear equations is the Harmonic Balance method with Newton-Raphson iteration. The time-marching tool used in calculations is the fourth-order Runge-Kutta method.

## GENERALIZED FLOQUET THEORY

### Floquet Theory

Floquet theory is one of the most powerful methods to obtain dynamic stability information for periodic problems; it is widely used to analyze the stability of helicopter rotors. The only requirements of Floquet analysis are time-marching tools and an eigenvalue solver. Floquet theory is an accurate method based on no assumptions or omissions. Its accuracy depends only on the time-marching tools and eigenvalue solver.

For linear differential equations with periodic coefficients such as:

$$\{\dot{x}\} + [D(t)]\{x\} = \{G(t)\} \quad (1)$$

where  $\{x\}$  is the state variable vector,  $[D(t)]$  is periodic coefficients with period  $T$ , and  $\{G(t)\}$  is the forcing function, the transient solution from  $t=0$  to  $t=T$  can be expressed in terms of the transition matrix  $[Q]$ :

$$\{x(T)\} = [Q]\{x(0)\} \quad (2)$$

$[Q]$  determines the stability of the system. Floquet's Theorem states that the transient solution has the form:

$$\begin{aligned} \{x(t)\} &= [A(t)]\{a_k \exp(\eta_k t)\} \\ &= [A(t)] \begin{bmatrix} \cdot & \cdot & \cdot \\ \cdot & \exp(\eta_k t) & \cdot \\ \cdot & \cdot & \cdot \end{bmatrix} \{a_k\} \end{aligned} \quad (3)$$

where  $A(t)$  is periodic. The  $\eta_k$  in the above equation are complex numbers. They can be expressed as:

$$\eta_k = \lambda_k + j\omega_k \quad (4)$$

Thus, instability occurs when  $\text{Re}(\eta_k) = \lambda_k > 0$ , which is equivalent to  $|\exp(\eta_k T)| > 1$ . The goal, therefore, is to find  $\exp(\eta_k T)$  from [Q].

In Eq. (3), one can see that

$$\{x(0)\} = [A(0)]\{a_k\}, \{a_k\} = [A(0)]^{-1}\{x(0)\} \quad (5)$$

A comparison of Eqs. (2) and (3) for arbitrary  $\{x(0)\}$ , along with the fact that  $[A(T)] = [A(0)]$  gives

$$[Q] = [A(0)] \begin{bmatrix} \ddots & & & \\ & \exp(\eta_k T) & & \\ & & \ddots & \\ & & & \ddots \end{bmatrix} [A(0)]^{-1} \quad (6)$$

or

$$\begin{bmatrix} \ddots & & & \\ & \exp(\eta_k T) & & \\ & & \ddots & \\ & & & \ddots \end{bmatrix} = [A(0)]^{-1} [Q] [A(0)] \quad (7)$$

Thus, one finds that  $\exp(\eta_k T)$  are the eigenvalues of [Q]; and  $[A(0)]$  are the eigenvectors. The characteristic exponents come directly from the natural log of the eigenvalues. For Fast Floquet Theory, T is replaced with T/Q; and the blade row partitions of [Q] are permuted before the eigenvalue calculation, Ref. [3].

Now, the only problem left is how to find the Floquet Transition matrix, [Q]. For perturbations about a periodic solution to a nonlinear differential equation:

$$\dot{x}_i = f_i(x_j, t) \quad (8)$$

if a small perturbation of x is added to the periodic solution,  $\bar{x}$ , then

$$\dot{\bar{x}}_i + \delta\dot{x}_i = f_i(\bar{x}_j + \delta x_j, t) \quad (9)$$

Thus we have a linearized set of equations about the periodic orbit

$$\delta\dot{x}_i = \left. \frac{\partial f_i(x, t)}{\partial x_j} \right|_{x=\bar{x}} \delta x_j \quad (10)$$

It follows that the partial derivative Jacobian in Eq. (10) is analogous to a [D(t)] in a linearized theory. Thus, numerical perturbations to  $\bar{x}(0)$  are

analogous to  $x(0)$  in the linear system; and perturbations to  $\bar{x}(T)$  are analogous to  $x(T)$ . Therefore, if one introduces a set of N independent perturbations; where N is the number of states:

$$[Perturbation]_{N \times N} = [\delta x_0^1, \delta x_0^2, \dots, \delta x_0^N]_{N \times N} \quad (11)$$

and then measures the perturbations in response at  $t=T$ ,

$$[Response]_{N \times N} = [\delta x_T^1, \delta x_T^2, \dots, \delta x_T^N]_{N \times N} \quad (12)$$

(where all perturbations are linearly independent), then one can compute the Floquet Transition matrix from the transient data.

$$[Q] = [Response] [Perturbation]^{-1} \quad (13)$$

With the help of an eigenvalue solver, it is then easy to determine the eigenvalues and stability. The above method could be used to do Floquet theory on a system provided that all states could be perturbed and all states measured. In some numerical codes, however, many states are simply ignored in the Floquet analysis (e.g., Ref.[9]). However, it is not always possible to predict *a priori* what states can be ignored. A more mathematically sound approach is needed.

### Generalized Floquet Theory

Floquet theory has stood out as the most powerful method to obtain dynamic information of periodic problems for more than thirty years since the first recorded paper of Lowis [1], and it is still widely used. McNulty's Fast Floquet Theory further improved the method. However, neither Fast Floquet theory nor Floquet Theory is practical when used to analyze larger systems or experimental data, since each method requires perturbations and measurements of all states. It is often difficult or even impossible to perturb and measure every state in a purely numerical simulation since even a simple rotor system might have hundreds of states. Therefore we look for a more practical and convenient method that can make tests simple and easy, a method that can give good accuracy but with efficiency.

Embedding theory offers a key. Those state vectors mentioned previously are state vectors in the current working space. If another working space can be constructed and the current space can be projected to the new working space by mapping, perhaps fewer

states can be considered in the new space. Obviously, the new space should contain the important modes and be orthogonal to unimportant modes. One commonly used method in nonlinear dynamics is to use the measured states (at  $t=0, T$ ) along with some time-shifted values of measured states (at  $t= \Delta t, T+\Delta t$ ) as the new working space, Refs. [5] and [10]. Time shifts are analogous to the use of higher derivatives of  $x(t)$ , but they are better conditioned than are finite-difference derivatives. As an example of pseudo states, consider that only  $x_1$  could be measured out of a list of states,  $x_n$ . The old state vector is  $X_{old}=[x_1, x_2, \dots, x_N]$ , and the new pseudo-state vector could be

$$X_{new}=[x_1(t), x_1(t+\Delta t), x_1(t+2\Delta t), \dots, x_1(t+(N-1)\Delta t)],$$

where  $\Delta t$  is the time shift. It is quite clear that with this method a set of states can be constructed very easily. The new method is named Generalized Floquet Theory

A very important question is, can these pseudo-states convey all the information needed to do stability analysis in the new space? The answer is yes, if they are properly chosen. Not only can such kind of information as  $\dot{x} \approx [x(t+\Delta t) - x(t)]/\Delta t$  be carried easily by  $x(t), x(t+\Delta t), \dots$ , but also flap states can carry lead-lag vibration information or inflow information. This is because many states in a system are connected closely by the structure, or airflow, or other media. Of course, some information (such as inflow information carried by blade states) might be weak; but, as long as good methods are applied, extraction of damping does not seem to be a big problem. This paper deals primarily with the pseudo-state method used to improve Floquet analysis. The Generalized Floquet Theory is still based on Floquet Theory and Fast Floquet Theory.

As an example, consider a system with only two states. The solution in Eq. (3) can be expressed as

$$\begin{bmatrix} x_1(t) \\ x_2(t) \end{bmatrix} = \begin{bmatrix} A_{11}(t) & A_{12}(t) \\ A_{21}(t) & A_{22}(t) \end{bmatrix} \begin{bmatrix} e^{\eta t} & 0 \\ 0 & e^{\eta_2 t} \end{bmatrix} \begin{bmatrix} a_1 \\ a_2 \end{bmatrix} = \begin{bmatrix} A_{11}(t) & A_{12}(t) \\ A_{21}(t) & A_{22}(t) \end{bmatrix} \begin{bmatrix} e^{\eta t} & 0 \\ 0 & e^{\eta_2 t} \end{bmatrix} \begin{bmatrix} A_{11}(0) & A_{12}(0) \\ A_{21}(0) & A_{22}(0) \end{bmatrix}^{-1} \begin{bmatrix} x_1(0) \\ x_2(0) \end{bmatrix} \quad (14)$$

Here,  $\begin{bmatrix} e^{\eta_1 T} & 0 \\ 0 & e^{\eta_2 T} \end{bmatrix}$  is the eigenvalue matrix of the Floquet Transition Matrix, and

$\begin{bmatrix} A_{11}(0) & A_{12}(0) \\ A_{21}(0) & A_{22}(0) \end{bmatrix}$  is the corresponding eigenvector matrix.

The Floquet Transition matrix in the original basis is given by:

$$Q_{old} = \begin{bmatrix} A_{11}(0) & A_{12}(0) \\ A_{21}(0) & A_{22}(0) \end{bmatrix} \begin{bmatrix} e^{\eta T} & 0 \\ 0 & e^{\eta_2 T} \end{bmatrix} \begin{bmatrix} A_{11}(0) & A_{12}(0) \\ A_{21}(0) & A_{22}(0) \end{bmatrix}^{-1} \quad (15)$$

Next, we change the current working space formed by state vector  $\begin{bmatrix} x_1(t) \\ x_2(t) \end{bmatrix}$  to a new working space formed by  $\begin{bmatrix} x_1(t) \\ x_1(t+\Delta t) \end{bmatrix}$ . This means the new space is formed from only one time-shifted original state. Application of Eq. (13) with a time shift gives:

$$\begin{bmatrix} x_1(t) \\ x_1(t+\Delta t) \end{bmatrix} = \begin{bmatrix} A_{11}(t) & A_{12}(t) \\ A_{11}(t+\Delta t)e^{\eta_1 \Delta t} & A_{12}(t+\Delta t)e^{\eta_2 \Delta t} \end{bmatrix} \begin{bmatrix} e^{\eta t} & 0 \\ 0 & e^{\eta_2 t} \end{bmatrix} \begin{bmatrix} a_1 \\ a_2 \end{bmatrix} = \begin{bmatrix} A_{11}(t) & A_{12}(t) \\ A_{11}(t+\Delta t)e^{\eta_1 \Delta t} & A_{12}(t+\Delta t)e^{\eta_2 \Delta t} \end{bmatrix} \begin{bmatrix} e^{\eta t} & 0 \\ 0 & e^{\eta_2 t} \end{bmatrix} * \begin{bmatrix} A_{11}(0) & A_{12}(0) \\ A_{11}(\Delta t)e^{\eta_1 \Delta t} & A_{12}(\Delta t)e^{\eta_2 \Delta t} \end{bmatrix}^{-1} \begin{bmatrix} x_1(0) \\ x_1(\Delta t) \end{bmatrix} \quad (16)$$

The Floquet Transition matrix in the new space is then

$$Q_{new} = \begin{bmatrix} A_{11}(0) & A_{12}(0) \\ A_{11}(\Delta t)e^{\eta_1 \Delta t} & A_{12}(\Delta t)e^{\eta_2 \Delta t} \end{bmatrix} \begin{bmatrix} e^{\eta T} & 0 \\ 0 & e^{\eta_2 T} \end{bmatrix} * \begin{bmatrix} A_{11}(0) & A_{12}(0) \\ A_{11}(\Delta t)e^{\eta_1 \Delta t} & A_{12}(\Delta t)e^{\eta_2 \Delta t} \end{bmatrix}^{-1} \quad (17)$$

Notice that the eigenvalues are the same as  $Q_{old}$  but the eigenvectors have changed since they are in the new space. There is a close relationship between those two spaces at the beginning or end of a period.

$$\begin{Bmatrix} x_1(T) \\ x_1(T+\Delta t) \end{Bmatrix} = [R] \begin{Bmatrix} x_1(T) \\ x_2(T) \end{Bmatrix} \quad (18)$$

$$[R] = \begin{bmatrix} A_{11}(0) & A_{12}(0) \\ A_{11}(\Delta t)e^{\eta_1 \Delta t} & A_{12}(\Delta t)e^{\eta_2 \Delta t} \end{bmatrix} \begin{bmatrix} A_{11}(0) & A_{12}(0) \\ A_{21}(0) & A_{22}(0) \end{bmatrix}^{-1} \quad (19)$$

This matrix  $\{R\}$  not only describes the relationship between those two spaces, but also determines the accuracy of further calculations. If this matrix has a zero eigenvalue, or is ill-conditioned, the new space could be missing vital information.

It is clear that the pseudo-state vector could be made up of any combination of the measurable states shifted by arbitrary amounts. For the studies in this section, we assume that the time shift  $\Delta t$  is the same for all shifted states and that it is an integer multiple of the smallest time unit in the problem,  $\delta t$  (time-marching step or sampling interval).

$$\Delta t = n \delta t \quad (20)$$

Therefore, if (for example) the flapping angle  $\beta$  were measured, then we could form states of

$$\{X\} = [\beta(t), \beta(t+\Delta t), \beta(t+2\Delta t), \beta(t+3\Delta t)\dots]^T \quad (21)$$

Figure 1 shows how the data are sampled:

Suppose the curve shown in the figure is the signal of flap vibration angle  $\beta$ . The first state vector used is  $[\beta_{11}, \beta_{21}, \beta_{31}, \beta_{41}]^T$ . It is a perturbation; its corresponding response after one period is  $[\beta_{12}, \beta_{22}, \beta_{32}, \beta_{42}]^T$ . If

$[\beta_{12}, \beta_{22}, \beta_{32}, \beta_{42}]^T$  is taken as another perturbation given at the end of the first period, the next response is  $[\beta_{13}, \beta_{23}, \beta_{33}, \beta_{43}]^T$ , and so on. The following equation shows how to form the new perturbation matrix and response matrix, and how to calculate new Floquet Transition matrix  $\{Q\}$ .

$$\begin{bmatrix} \beta_{12} & \beta_{13} & \beta_{14} & \beta_{15} \\ \beta_{22} & \beta_{23} & \beta_{24} & \beta_{25} \\ \beta_{32} & \beta_{33} & \beta_{34} & \beta_{35} \\ \beta_{42} & \beta_{43} & \beta_{44} & \beta_{45} \end{bmatrix} = [Q] \begin{bmatrix} \beta_{11} & \beta_{12} & \beta_{13} & \beta_{14} \\ \beta_{21} & \beta_{22} & \beta_{23} & \beta_{24} \\ \beta_{31} & \beta_{32} & \beta_{33} & \beta_{34} \\ \beta_{41} & \beta_{42} & \beta_{43} & \beta_{44} \end{bmatrix} \quad (22)$$

$$\{Q\} = [\text{Response}] [\text{Perturbation}]^{-1} \quad (23)$$

It is easy to see that more pseudo-states could be added to the state vectors by adding more time shifts (i.e., add more rows to the perturbation and response matrices). Similarly, more couples of perturbations and measurements could be added to the above equations by taking more periods (i.e., add more

columns to the perturbation matrix and response matrix). Thus, the new Floquet Transition matrix may not be of the same size as the old one. If the Floquet Transition matrix is larger than the old one, then zero or very small (almost zero) eigenvalues will be found corresponding to infinitely damped numerical modes. They are physically meaningless. If the Floquet Transition matrix is smaller than the old one, this means some information is missing in the new state space. Thus, the accuracy will be determined by the nature of the neglected directions in state-space.

Selection of different parameters can give different accuracy or even different results. Initial calculations for the one-bladed system in this research give the following results:

1. The smaller  $\delta t$  is, the better the result is.
2. The choice  $X = \beta, \dot{\beta}$  gives more accurate flap damping; and the choice  $X = \zeta, \dot{\zeta}$  gives more accurate lag damping.
3. Solutions achieve good accuracy when time delay  $\Delta t = n\delta t$  is selected to give a well-conditioned Relation matrix

The explanation for the first conclusion is that time-marching is more accurate with a smaller step size. The explanation of the second conclusion is that flap and lag vibrations are lightly coupled together by the structure and static inflow. Lead-lag vibration information carried by flap states may be weak, but it is enough to give good results. That is why selecting  $X = \beta, \dot{\beta}$  gives more accurate flap damping, while selecting  $X = \zeta, \dot{\zeta}$  give more accurate lag damping.

The third conclusion as to which time delay factor  $n$  should be used for  $\Delta t = n\delta t$  is a little difficult to decide since it is affected by the coupling of vibrations and structural characteristics as well as selection of the pseudo spaces. However, it is possible to select a better time delay factor based on information given by the relation matrix. A good time delay factor is one that corresponds to a good relation matrix, so something reflecting the quality of the relation matrix can be used as a criterion. The condition number of the relation matrix is a possibility. It is defined as the ratio of the largest singular value of the matrix to the smallest one. It will be mentioned in detail later.

### An Example

In order to give a preliminary comparison, a simple example is given. The following is the calculation result of a one-bladed system with no inflow. The pseudo-state vector is  $\{X\} = [\beta(t), \beta(t+\delta t), \beta(t+2\delta t), \beta(t+3\delta t)]^T$ , only  $\beta$  is

excited and measured; the time delay is  $\Delta t = 2\pi/64$  (time delay factor  $n=1$ ). Results are shown in Figure 2. Both lag damping and flap damping curves are shown versus advance ratio,  $\mu$ . The other parameters are :

$$P=4/3, W=2, Z=0, \gamma=5, C_{d_0}=0.01, C_{\zeta}=0, C_{\tau}=0.01, \sigma=0.05, a=2\pi, \beta_s=\beta_c=0.$$

For detailed equations, see Ref. [11].

Note that the pseudo-state results are indistinguishable from the conventional Floquet results. The maximum relative lag damping error of the Generalized Floquet Theory is 0.13% (near to where lag damping crosses zero line); the max relative flap damping error is  $8.6 \times 10^{-5} \%$  since the flap damping is far away from zero.

This simple example clearly shows how good the Pseudo-State method can be. The introduction of Pseudo-States can make some information weak and thus can reduce the accuracy of calculation; but the accuracy is good enough here to give a satisfactory answer. These errors become larger when we include dynamic inflow states but do not measure dynamic inflow. Errors also become larger when all states cannot be perturbed. Further discussion of numerical methods that can be used to reduce error will be mentioned later.

Generally speaking, the pseudo-state method is a practical improvement that can be applied either to Floquet Theory or to Fast Floquet Theory. Its application is of great importance to stability testing. By a simple replacement of the real states with pseudo-states, many difficult problems can be solved with ease. Current measurement techniques do not measure inflow states. Most applications of Floquet theory to large rotorcraft simulations also ignore inflow states, Ref. [9]. The results have not been satisfactory. With conventional techniques, it is difficult to perturb and measure all blade states. A simple rigid-bladed rotor model for 4-bladed system has 16 blade states, a complicated flexible rotor system may have hundreds or thousands of states that need to be tested. It is not feasible to attach hundreds and thousands of sensors to a single rotor. The following section will discuss accuracy issues and enhancement methods for more challenging examples.

## ACCURACY AND ADVANCED METHODS

### Four-Bladed Rotor System

In order to test the new method on a more challenging example, a four-bladed system with

dynamic wake is used. Parameters are the same as for the one-bladed system.

$$C_{\zeta} = 0, C_{d_0} = 0.01, C_{\tau} = 0.01, \sigma = 0.05, a = 2\pi, \gamma = 5, P = 4/3, W = 2, \mu = 0, \beta_c = \beta_s = 0$$

The dynamic inflow model calculation is Peters' model described in Ref. [8]. Fifteen inflow states (4 harmonics) are used, plus  $4 \times 4 = 16$  blade states. The total number of all states used is 31. This means the Floquet Transition matrix is  $31 \times 31$ . Both Floquet and Fast Floquet methods are used. Damping is identical by either method, but frequency is more uniquely defined by Fast Floquet Theory. Thus all results shown are for Fast Floquet Theory. Solutions are expressed in the form of complex numbers. Negative real parts of the complex numbers are damping, imaginary parts are the corresponding frequencies. The system is unstable if any damping is negative. (Positive damping means vibration energy is being taken out of the system, so the system vibration will decrease with increasing time; negative damping means the vibration energy of the corresponding mode is increasing.)

The system has two principal kinds of vibrations: flap vibration and lead lag vibration. Every kind of vibration has four different rotor modes, Ref. [12]:

- progressive mode---vibration amplitudes rotate in the same direction as the rotor
- regressive mode--- vibration amplitudes rotate in the opposite direction as the rotor
- differential mode---two blades vibrate in one direction and the other two in the opposite direction.
- collective mode---all four blades vibrate in the same direction.

The system has totally 31 eigenvalues. Calculation results given by the pseudo-state method may have more or fewer damping values depending on the number of states and perturbations. If the new Floquet Transition matrix is larger than  $31 \times 31$ , extra eigenvalues are likely to be large negative numbers. Full Floquet is used to identify exact results for the error analysis.

In order to identify a certain set of excitations and measurements, we introduce the following notations:

E---implies which states are excited to obtain data

M---implies which states are measured in data

For example, E $\beta$ -8 implies that only  $\beta_i$ 's are given a non-zero initial condition. However, the response is allowed to go through 8 blade passages so that 9 columns of data (8 pairs) can be used as input

and output data columns for  $\beta_i$ . Similarly  $M\beta$ -8 implies that 8 pseudo states are measured:  $\beta(t)$ ,  $\beta(t+\Delta t)$ ,  $\beta(t+2\Delta t)$ ,  $\beta(t+3\Delta t)$ ,  $\beta(t+4\Delta t)$ ,  $\beta(t+5\Delta t)$ ,  $\beta(t+6\Delta t)$ ,  $\beta(t+7\Delta t)$ . The same notation is used for  $\dot{\beta}$ ,  $\zeta$ ,  $\dot{\zeta}$ , etc. with the appropriate symbol used in place of  $\beta$ .

The introduction of pseudo-states may give the impression that pseudo-states can be chosen arbitrarily. However, this is not the case. If only one blade state is perturbed and measured, some useful information will be very weak, and the accuracy of calculation can suffer. Sometimes several damping values may be missing. So it is still very important to select pseudo-states carefully.

### An Example:

One of the most obvious factors noted in Ref.[11] is that one should measure and excite the same physical variable. Second, we find that both  $\beta$  and  $\zeta$  should be used. Third, it is also noted that displacements are better than velocities. Therefore, we come to the conclusion that a good pseudo-state selection might be  $E\beta, \zeta$ -4,  $M\beta, \zeta$ -4. This gives a  $32 \times 32$  matrix with both  $\beta$  and  $\zeta$ . Table 1 shows how this approach can give good accuracy. Once again,  $n=1$  so that  $\Delta t = \delta t = 2\pi/64$ .

Now we see that errors are larger than for the one-bladed system with no inflow. This is because the model is more complicated with inflow. However, the only errors that are even moderately large are regressive lag damping (12.6%) and regressive flap frequency (15.9%). Note, however, that for these two numbers the true values are small (0.0089 and 0.1184), so that even small absolute error can give moderately large percentage error. Therefore, the results are all very good. Since blade states  $\beta$  and  $\zeta$  are what one would usually measure in an experiment, and since inflow states are often impossible to measure directly, the example shows that the most physically obvious choice for pseudo-states is quite good even with no optimization of time shift (the smallest step is used).

It is now interesting to compare that result with what is presently done in large codes such as UMARC, Ref. [9]. In those codes, although inflow states are included in the simulation, they are ignored in Floquet. This is equivalent in our notation to the use of  $E\beta, \zeta, \dot{\beta}, \dot{\zeta}$ -1,  $M\beta, \zeta, \dot{\beta}, \dot{\zeta}$ -1. Table 2 shows the error in the eigenvalues under that older approach. One can see that the errors are several times larger than those in Table 1 with damping

errors from 20% to almost 50%. This shows the tremendous improvements that can be made with the pseudo-state method even when it does not utilize  $\dot{\beta}$  and  $\dot{\zeta}$ .

### Time Delay

In the previous result, the time delay used for pseudo-states is based on the smallest time step available. Time delay is a very important parameter, and it directly controls the data sampling and distribution. Therefore, it might be that other time delays are even better. If damping and frequencies are all considered as information of the system, the best pseudo-state selection is one that can carry as much useful information as possible. From Figure 1, it is not difficult to see how some data can be wasted if  $\beta_{11}, \beta_{21}, \beta_{31}, \beta_{41}$  are too close to each other. In other words, there can still be much data left unused. In order to separate those pseudo-states and obtain a better pseudo-state distribution, a larger time delay could be used. As defined previously, the time delay  $\Delta t$  is the product of time delay factor  $n$  and the smallest time unit  $\delta t$ . The smallest time unit cannot be changed if time-marching is completed or the sampling rate is selected. However, the time delay factor can be changed easily. The larger the time delay factor, the more scattered are the pseudo-states. However, if a time delay is too large, a pseudo-state vector may be extended into the next blade passage. This would decrease information, since the next blade passage is being sampled separately. Thus, the best time delay factor depends on the system, the pseudo-state selection, and other parameters. It is difficult to say which is the best without any calculations. However, one might expect that for  $M\beta, \zeta$ - $k$ ,  $E\beta, \zeta$ - $k$ , one would want  $\Delta t < 2\pi/[(k-1)Q]$  to keep all measurement in one blade passage, and  $\Delta t = 2\pi/(kQ)$  to keep all measurements equally spaced from one blade passage to the next.

The following example will show how important the time delay factor is. Table 3 is for the case  $E\beta, \zeta$ -4,  $M\beta, \zeta$ -4, which is a good pseudo-state selection. In this case (and all other 4-bladed modal cases),  $\delta t = 2\pi/64$ . Thus, there are 16  $\delta t$  steps in a blade passage.

Even though  $E\beta, \zeta$ -4,  $M\beta, \zeta$ -4 is a good pseudo-state selection, its result can still be improved from 3% error down to less than 2% by a change in the time delay factor  $n$  from 1 to 5. It is interesting that, for  $M\beta, \zeta$ -4, one measures through 3  $\Delta t$ 's. Thus, for  $n=5$ , one measures through 15  $\delta t$ 's which keeps all measurements within one blade passage (16

$\delta t$  steps). The equally-spaced choice,  $\Delta t = 2\pi/kQ = 4\delta t$  ( $n=4$ ), does not seem to give as good of a result. The  $n=5$  result is actually better. This might be due to the fifth point being close to the first point on the next blade passage. Interestingly, the choice  $\Delta t = 2\delta t$ , which is one-half of the equally-spaced value, keeps all measurements in the first one-half blade passage and gives good results.

### Least Squares Method

The Least Squares method is a method that can be used to reduce errors, especially errors produced by random variations in the data. Thus, it is applicable with the pseudo-state method. The application of the method takes place when the number of excitations is not equal to the number of pseudo-states. Then, instead of a normal inverse, a least-squares (or generalized) inverse must be used and equation (13) becomes:

$$[Q]=[Response] [Perturbation]^+ \quad (24)$$

where "+" means the generalized inverse based on singular value decomposition. Please refer to Ref. [13] for details.

The following example, Table 4, is one that uses the Least Squares method when the number of pseudo-states is increased to more than the number of excitations. The time delay is  $n=1$ .

One can see that, as more measurements are added, the error decreases due to the use of the additional information. A similar example in Ref. [11] shows that increasing the number of excitations also gives better results.

### Relation Matrix

So far, good accuracy has been achieved; and we have a general impression of how to improve the pseudo-state method. However, we now wish to understand why some parameter combinations give better accuracy than others. The key is in the Relation matrix.

The Relation matrix is defined as the product of two eigenvector matrices. That is:

$$[R]=\begin{bmatrix} \text{Eigenvector Matrix of} \\ \text{New Floquet Transition Matrix} \end{bmatrix} * \begin{bmatrix} \text{Eigenvector Matrix of} \\ \text{Old Floquet Transition Matrix} \end{bmatrix}^{-1} \quad (25)$$

and it is also expressed as:

$$[\text{New Pseudo-State Vector}] = [R][\text{Old State Vector}] \quad (26)$$

So, the Relation matrix is obviously very important. It determines the quality of the mapping from the old space to the new space. It also determines the error caused by the mapping. If the rank of the Relation matrix is smaller than the number of states used in the old state vector, the mapping may introduce errors.

What we need is some indicator that can estimate the error of the pseudo-state method. This indicator must have some correspondence with the relation matrix. It could be the singular values of the relation matrix or something else. Here, we use the condition number to indicate the quality of the relation matrix. Condition number is a commonly used parameter to indicate the quality of a matrix. It is defined as the ratio of the largest singular value to the smallest. It is infinite if the matrix is singular. Therefore, the smaller the condition number is, the better the matrix is. The following example will show how well the condition number of the Relation matrix is related to accuracy. However, condition number is only one aspect of the Relation matrix. To find more about the Relation matrix, we need to examine all singular values.

Figure 3 gives an example that clearly shows the correlation between condition number of the Relation matrix and relative error. A 4-bladed rotor system with dynamic inflow is used ( $\mu=0$ ). In this case, all blade states are excited but only  $\zeta$  is measured.

The horizontal coordinate is time delay factor,  $n$ . One curve is the log of the condition number of the Relation matrix, and the other curve is the log of average total error. Those two curves have the same general up and down trends. This clearly demonstrates the previous conclusion.

However, as mentioned earlier, the eigenvector matrix of old Floquet Transition matrix is not available unless the exact result is known. This means that the Relation matrix is not available for testing, and it can not be used as a rule. The reason we use it is that it can help find out more about the new method and the system. Though the relation matrix is not available for testing, the eigenvector matrix of the new Floquet Transition matrix is available, and it contains most of the error information carried by the Relation matrix. So, further work needs to be done to find out whether the condition number of the eigenvector matrix of new Floquet Transition matrix can be used as a rule.

## Weak Information, Error and Noises

Error and weak information have been shown to be the major sources of error. It seems that selection of good pseudo-states can help solve these problems, but 2% error is not perfect for flap and lag eigenvalues, and we would like to find inflow damping. So, it is necessary to improve the method further. In real experiments, error comes partially from noise. People often solve this problem by using some filters to filter high frequency or low frequency noise. For us, noise is unavoidable since the pseudo-state method itself is designed to analyze experimental data. Currently, the error mainly comes from the calculation procedure; but it is not a bad idea to try to eliminate poor data before it enters the transition matrix.

An obvious tactic is to use Singular Value Decomposition. The perturbation matrix and response matrix need to be examined for their singular values, and small values need to be eliminated. (For a detailed description of Singular Value Decomposition, see Ref. [11].)

In this method, Eq. (22) is generalized. If we have some measurements such that

$$[R]=[Q][P] \quad (27)$$

where R=response and P=perturbation, then a SVD is done for both [R] and [P] matrices.

$$[V]^T [P] [U] = \begin{bmatrix} p_1 & 0 & 0 \\ 0 & \ddots & 0 \\ & 0 & p_n \\ 0 & & 0 \\ 0 & & 0 \\ 0 & \dots & 0 \\ 0 & \dots & 0 \end{bmatrix} \quad (28)$$

$$[Y]^T [R] [W] = \begin{bmatrix} r_1 & 0 & 0 \\ 0 & \ddots & 0 \\ & 0 & r_n \\ 0 & & 0 \\ 0 & & 0 \\ 0 & \dots & 0 \\ 0 & \dots & 0 \end{bmatrix} \quad (29)$$

where U,V,Y, and W are unitary. Some values of  $p_i$  or  $r_i$  may be numerically very small, and these are set identically to zero. (i.e., treated as zero singular values). Then, [Q] is formed from the generalized inverse of P.

$$[Q]=[R] [P]^* =$$

$$[Y] \begin{bmatrix} r_1 & 0 & 0 \\ 0 & \ddots & 0 \\ & 0 & r_n \\ 0 & & 0 \\ 0 & & 0 \\ 0 & \dots & 0 \\ 0 & \dots & 0 \end{bmatrix} [W]^T [U] \begin{bmatrix} \frac{1}{p_1} & 0 & 0 & 0 & 0 \\ 0 & \ddots & 0 & & \\ & 0 & \frac{1}{p_n} & & \\ 0 & & 0 & & \\ & & & 0 & 0 & 0 \end{bmatrix} [V]^T \quad (30)$$

The truncated  $p_i$  or  $r_i$  remove extraneous rows from Y, W, or U, V.

The ignored data represent zero eigenvalues of [Q] which are physically meaningless, infinite-damping modes. Moreover, [Q] can be reduced explicitly to a matrix having the smaller rank of  $r_i$  or

$p_i$ . Thus, the least squares method used earlier is a special case of Eqs (28)-(30) for which no  $p_i$  is zero.

In the previous data, some very small singular values of the perturbation matrix and response matrix exist. Some of those are almost zero. Final calculations show that the smaller values contain more noise than useful information, and they really should be truncated, but the larger ones contain more useful information and should be kept. The smallest singular value is smaller than 1 millionth of the largest one.

There are two ways to truncate the vector associated with the smaller singular values. One is to put the perturbation matrix and response matrix together, find the composite singular values, and truncate the smaller ones no matter from which matrix they originated. The other is to truncate the smaller singular values of the perturbation matrix and those of the response matrix separately.

The truncation number is defined as the number of smaller singular values truncated. The following example is done using  $E\beta, \zeta -4$ ,  $M\beta, \zeta -4$ , and a time delay factor  $n=1-8$  (time delay  $\Delta t = (1-8) \times 2\pi / 64$ ). Smaller singular values of the perturbation matrix and of the response matrix are treated the same.

The 8 curves in Figure 4 represent 8 data lines for delay factors  $n=1-8$ . Error is plotted versus the number of small singular values that are set to zero (truncated). The best result is 1.36% error when delay =2, truncation number =13. This is less than the 1.93% error when no smaller singular values are truncated. Notice also that most of the improvement comes when the 7 smallest singular values are truncated, and little more is gained when the next 8-16 are truncated. Thus, the general pattern of keeping larger singular values seems to work well. Time shifts with the larger original errors are most helped

by truncation. Thus, the  $n=2$  and  $n=5$  results are not greatly improved by truncation, but  $n=7$  is greatly improved. This indicates that the error due to poor time shifts is in lower singular values. All time shifts show deteriorated results when more than 20 singular values are truncated.

The following are some conclusions summarized from the last three examples:

1. Some singular values are nearly zero; they are generated by calculation errors and should be truncated.
2. Truncation of small singular values of the perturbation matrix and response matrix separately gives better results than treating them both as a single matrix to be decomposed.
3. Truncation of some larger singular values can reduce the error of one damping while increasing the error of another.

### Inflow Damping

The inflow damping cannot be measured easily in experiments due to the limitations of current testing techniques. The pseudo-state method offers a possible way to find inflow damping. Thus far, we have optimized results based on flap and lag eigenvalues. Now, we see if present methods are enough to give inflow damping for the least-damped inflow mode.

Figure 5 shows results with  $E\beta, \zeta -8, M\beta, \zeta -8$ , which results in a  $64 \times 64$  Floquet Transition matrix and 128 singular values from the perturbation matrix and the response matrix. Cases are shown for time shifts from 1 to 4. Note that for this case ( $k=8$ ), the  $n=3$  and 4 cases bring measurements into the next blade passage. Since the four-bladed system has only 31 states, the first 66 smaller singular values ( $64 \times 2 - 31 \times 2 = 66$ ) contain much noise. Nevertheless, one or two truncations brings  $n=3$  and  $n=4$  down to very small errors; and about 8 more truncations brings  $n=2$  down to small errors. The case of  $n=1$  (smallest shift) is only accurate when nothing is truncated.

This is a satisfying result. Any answer within 20% should be considered good for very highly damped inflow modes that are not being measured directly. There is also some inflow data in the smaller singular values; but it is often not accurate enough to keep.

### SUMMARY AND CONCLUSIONS

A new method of Generalized Floquet Theory has been introduced. In this method, it is assumed that only some states are measured for a limited

number of initial conditions. More initial conditions are generated by consideration of each experiment (numerical or physical) through more blade passages. More states are brought out (pseudo-states) through time shifts ( $\Delta t$ ) that keep all shifts within a given blade passage. The so-expanded data are analyzed through singular-value decomposition to obtain the best estimate of the Floquet Transition Matrix.

Generalized Floquet Theory is an improvement to either Floquet Theory or Fast Floquet Theory and has direct application to helicopter stability testing. Unmeasurable states can be replaced with pseudo-states; and difficult problems, such as how to find inflow damping by experiment, can be solved. It also helps to make the experiment easy since only a few states need to be perturbed and measured. This is an improvement that could save time and money. Therefore, it is a very practical and useful method.

Generalized Floquet Theory brings convenience and new ideas to solve tough problems that could not otherwise be treated. The conceptual difference between Floquet Theory (Fast Floquet Theory) and Generalized Floquet Theory is that Floquet Theory uses only very strong information. It gives erroneous results if any states are ignored. Generalized Floquet Theory utilizes all information (strong information and weak information) carried by the pseudo-states even with measurement noise.

Singular Value Decomposition with a generalized inverse is like the Least Squares Method except that extraneous singular values can be discarded prior to processing. This method, along with the time delay, improves results. It is also found that the Relation Matrix, which clearly indicates the relation between the new state vector and old state vector, can be used in some way to help understand more about the system.

Several examples are given in this paper to show the effectiveness of the pseudo-state method. It is also found that inflow damping, which is calculated from very weak information by pseudo-states, can be found with fair accuracy. Comparing this with current techniques, the pseudo-state method reaches a higher level of accuracy than that can be found with current techniques. It is found that it is important to be able to measure the displacement (but not necessarily velocities) of important states. The work further shows that all shifts should be kept in one blade passage but not spread evenly over the passage. A good shift seems to be  $\Delta t = 2\pi / (2kQ)$  where  $Q$  is the number of blades and  $k$  is the number of pseudo states per measured variable (time shift plus one). The work further shows that only the very smallest singular values of the perturbation need to be truncated.

Further research work to improve accuracy is still necessary. Further research work to try this method and summarize practical experiences is also necessary. Another very useful idea is that, since the pseudo-state method utilizes all kinds of information with noise, then noise might be filtered by some numerical filters and thus good accuracy can be achieved. This idea may provide a good direction for future research. Future research will also focus on finding ways of error estimation.

### References

[1] Lowis, O. J., "The Stability of Rotor Blade Flapping Motion at High Tip Speed Ratios," Reports and Memoranda No. 3544, Jan 1963 .

[2] Peters, David A., and Hohenemser Kurt H., "Application of the Floquet Transition Matrix to Problems of Lifting Rotor Stability," *Journal of the American Helicopter Society*, Vol. 16, No. 2, April 1971, pp. 25-33.

[3] Peters, David A., "Fast Floquet Theory and Trim for Multi-Bladed Rotorcraft," Proceedings of the 51<sup>st</sup> Annual Forum of the American Helicopter Society, Fort Worth, TX, May 1995, pp. 444-460.

[4] Peters, David A., and Su, Ay, "The Effect of Hidden Dynamic States of Floquet Eigenvalues," *Journal of the American Helicopter Society*, Vol. 35, No. 4, Oct 1990, pp. 72-75.

[5] Bayly, P. V. and Virgin, L. N., "An Empirical Study of the Stability of Periodic Motion in the Forced Spring-pendulum," Proceedings of the Royal Society of London, 443A: pp391--408, 1993.

[6] Wang, Xin, and Peters, David A. "Floquet Analysis in the Absence of Complete Information on

States and Perturbations," Proceedings of the Seventh International Workshop on Dynamics and Aeroelastic Stability Modeling of Rotorcraft Systems, Oct 1997, St. Louis, MO.

[7] Peters, David A., "Flap-Lag Stability of Helicopter Rotor Blades in Forward Flight," *Journal of the American Helicopter Society*, Vol. 20, No. 4, October 1975, pp. 2-13.

[8] Peters, David A., Boyd, David D., and He, Cheng Jian, "Finite-State Induced-Flow Model for Rotors in Hover and Forward Flight," *Journal of the American Helicopter Society*, Vol. 34, No. 2, April 1989, pp. 5-17.

[9] Bir, G., and Chopra, I., "Status of University of Maryland Advanced Rotorcraft Code (UMARC)," Proceedings of the Aeromechanics Specialists Conference, San Francisco, January 19-21, 1994, Paper PS. 5.

[10] Nayfeh, Ali H. and Balachandran, Balakumar, *Applied Nonlinear Dynamics*. New York, Published by John Wiley & Sons, 1995, pp.478.

[11] Wang, Xin, The Method of Generalized Floquet Theory Applied to Flap-Lag Dynamics with Inflow, Master of Science Thesis, Washington University in St. Louis, May 1998.

[12] Peters, David A., and Su, Ay, "Effect of an Unsteady Three-Dimensional Wake on Elastic Blade-Flapping Eigenvalues in Hover," *Journal of the American Helicopter Society*, Vol. 38, No. 1, Jan. 1993, pp 45-54.

[13] Atkinson, Kendall E., *An Introduction to Numerical Analysis, Second Edition*. New York, Published by John Wiley & Sons, 1989, pp.478, pp.636.

Table 1 Data Analysis for Case E  $\beta, \zeta -4, M \beta, \zeta -4$

		Exact Fast Floquet Solutions	E $\beta, \zeta -4$ M $\beta, \zeta -4$	Damping Error (%)	Frequency Error (%)	Average Error (%)
Lead-Lag Damping + Frequencies	Regressive	-0.0089 + 0.4196i	-0.0078 + 0.4165i	12.55	0.75	6.65
	Differential	-0.0109 + 0.5882i	-0.0103 + 0.5891i	5.37	0.16	2.77
	Progressive	-0.0071 + 1.5880i	-0.0074 + 1.5901i	3.66	0.14	1.90
	Collective	-0.0067 + 1.4156i	-0.0066 + 1.4126i	2.28	0.21	1.25
<b>Average Lead-Lag Damping + Frequency Error</b>						<b>3.14</b>
Flap Damping + Frequencies	Regressive	-0.1699 + 0.1022i	-0.1734 + 0.1184i	2.08	15.93	9.00
	Differential	-0.2715 + 0.8323i	-0.2800 + 0.8294i	3.10	0.34	1.72
	Progressive	-0.2915 + 1.8667i	-0.2880 + 1.8587i	1.22	0.43	0.82
	Collective	-0.2699 + 1.0887i	-0.2703 + 1.0936i	0.17	0.45	0.31
<b>Average Flap Damping + Frequency Error</b>						<b>2.96</b>
<b>Average Damping + Frequency Error</b>						<b>3.05</b>

Table 2 Error of Previous Approach,  $E \beta, \zeta, \dot{\beta}, \dot{\zeta} -1, M \beta, \zeta, \dot{\beta}, \dot{\zeta} -1$

		Exact Fast Floquet Solutions	$E \beta, \zeta, \dot{\beta}, \dot{\zeta} -1, M \beta, \zeta, \dot{\beta}, \dot{\zeta} -1$	Damping Error (%)	Frequency Error (%)	Average Error (%)
Lead-Lag Damping + Frequencies	Regressive	-0.0089 + 0.4196i	-0.0079 + 0.4160i	11.66	0.85	6.25
	Differential	-0.0109 + 0.5882i	-0.0086 + 0.5851i	21.50	0.52	11.01
	Progressive	-0.0071 + 1.5880i	-0.0088 + 1.5861i	23.60	0.11	11.86
	Collective	-0.0067 + 1.4156i	-0.0089 + 1.4148i	33.38	0.05	16.72
<b>Average Lead-Lag Damping + Frequency Error</b>						<b>11.46</b>
Flap Damping + Frequencies	Regressive	-0.1699 + 0.1022i	-0.2527 + 0.1107i	48.78	8.32	28.55
	Differential	-0.2715 + 0.8323i	-0.2563 + 0.8765i	5.60	5.32	5.46
	Progressive	-0.2915 + 1.8667i	-0.2607 + 1.8699i	10.57	0.17	5.37
	Collective	-0.2699 + 1.0887i	-0.2517 + 1.1210i	6.75	2.97	4.86
<b>Average Flap Damping + Frequency Error</b>						<b>11.06</b>
<b>Average Damping + Frequency Error</b>						<b>11.26</b>

Table 3 Case  $E \beta, \zeta -4, M \beta, \zeta -4$  with Various Time Delay Factors  $n$

Time delay $\Delta t = n \frac{2\pi}{64}$	Average Lag Error (%)	Average Flap Error (%)	Average Error (%)
Time delay factor $n=1$	3.14	2.96	3.05
Time delay factor $n=2$	3.32	0.66	1.98
Time delay factor $n=3$	3.58	4.02	3.80
Time delay factor $n=4$	4.94	2.20	3.57
Time delay factor $n=5$	2.64	1.22	1.93
Time delay factor $n=6$	2.93	4.37	3.66
Time delay factor $n=7$	2.34	6.53	4.43
Time delay factor $n=8$	2.00	3.85	2.93

Table 4 The Effect of Increased Number of Pseudo-States By the Least Squares Method

Excitations	Measurements	Average Error of lag damping and frequencies (%)	Average Error of flap damping and frequencies (%)	Average Error (%)
$E \beta, \zeta -4$	$M \beta, \zeta -4$	3.14	2.96	3.05
$E \beta, \zeta -4$	$M \beta, \zeta -8$	3.70	1.30	2.50
$E \beta, \zeta -4$	$M \beta, \zeta -16$	2.61	1.58	2.10
$E \beta, \zeta -4$	$M \beta, \zeta -24$	2.40	1.98	2.19
$E \beta, \zeta -4$	$M \beta, \zeta -32$	2.16	0.67	1.42
$E \beta, \zeta -4$	$M \beta, \zeta -40$	2.27	0.78	1.52

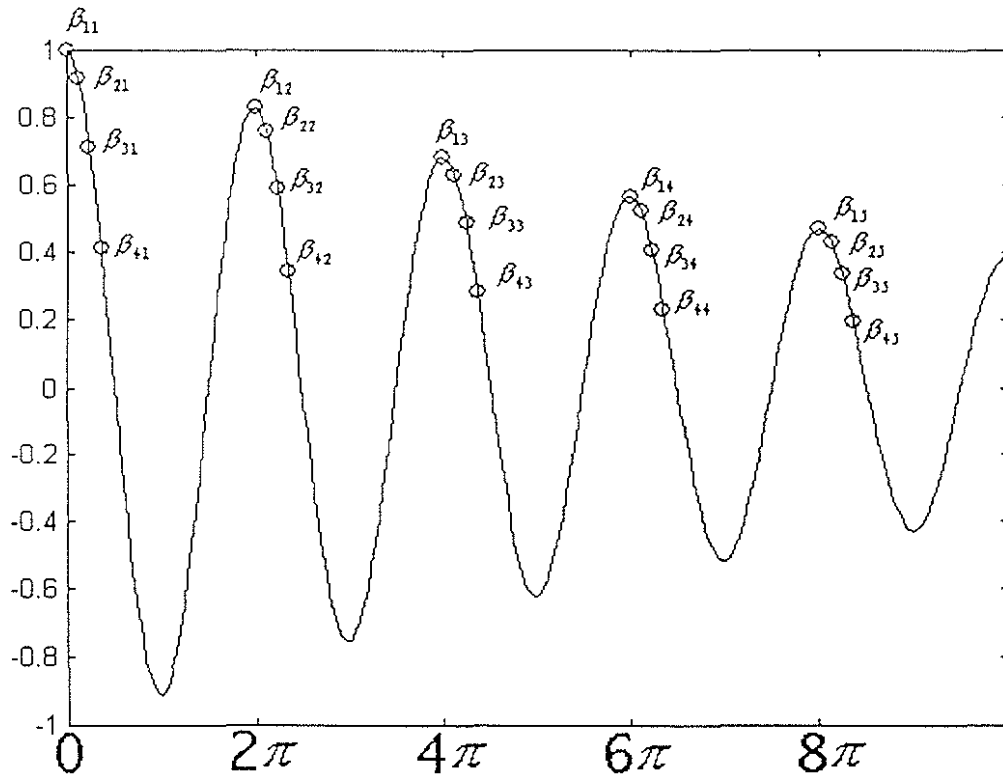


Figure 1 Sampling Data Using the Pseudo-State Method

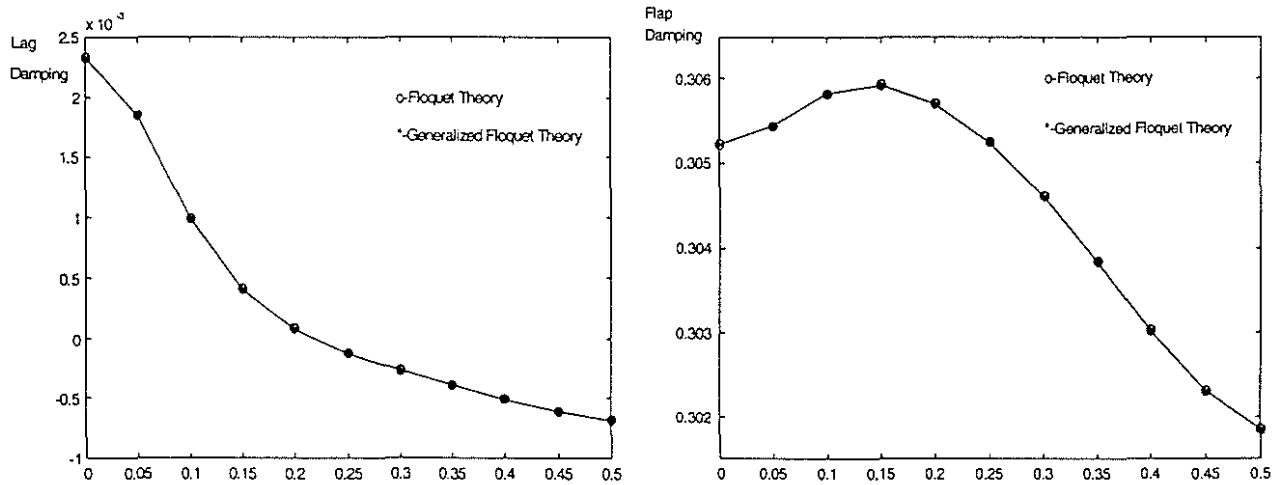


Figure 2 Accuracy of the Pseudo-State Method (Generalized Floquet Theory)

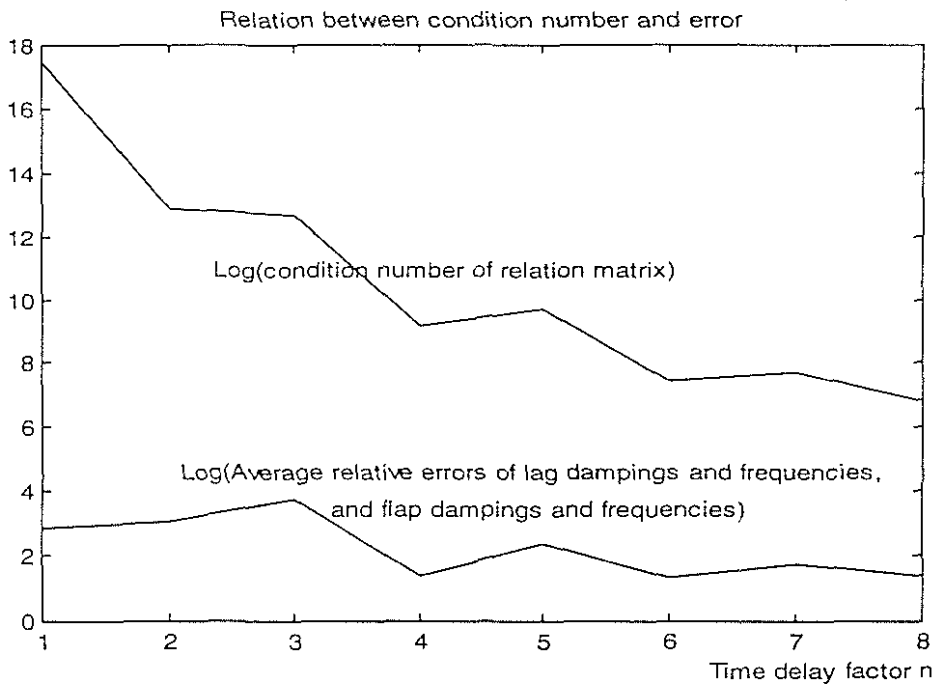


Figure 3 Condition Number of Relation Matrix and Average Error

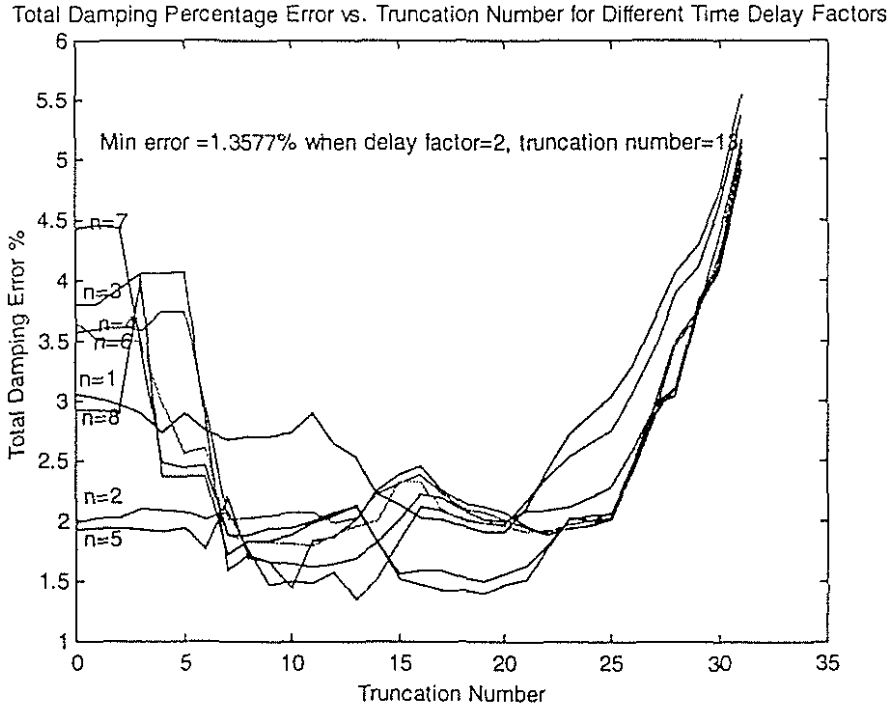


Figure 4 Total Damping Percentage Error vs. Truncation Number for Different Time Delay Factors

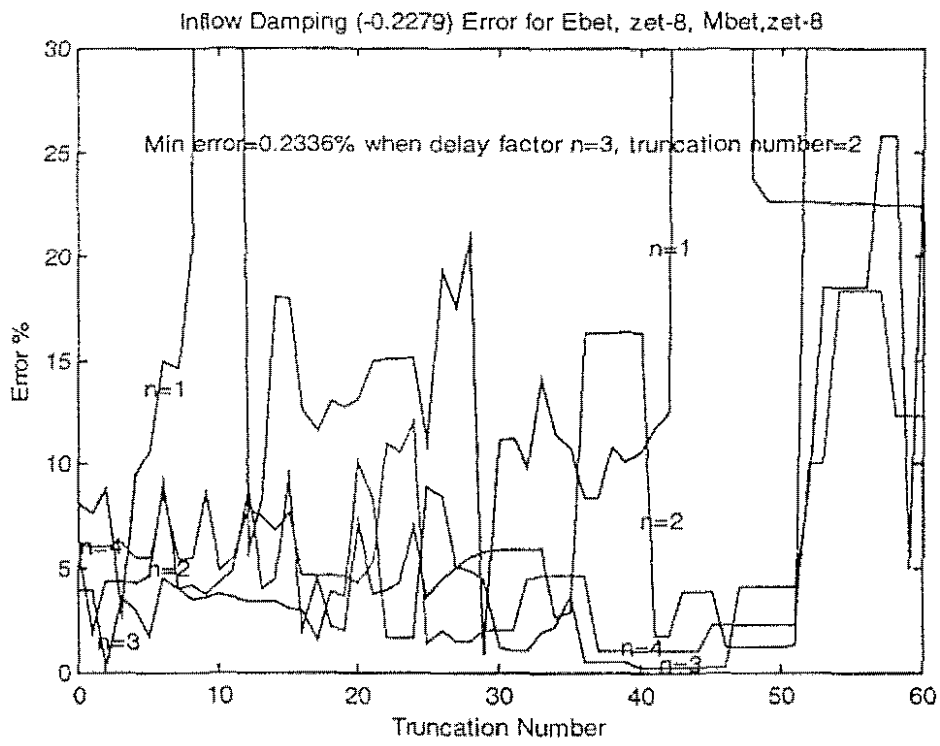


Figure 5 Inflow Damping